

Negative correlation peak shaving control in a parking garage in Uppsala, Sweden

Alexander Wallberg^{*}, Valeria Castellucci, Carl Flygare, Emil Lind, Egil Schultz, Marina Martins Mattos, Rafael Waters

Division of Electricity, Department of Electrical Engineering, Uppsala University, Box 65, Uppsala, 75103, Sweden

ARTICLE INFO

Keywords:

Peak shaving
Negative correlation
Mobility house
Genetic algorithm
Dansmästaren

ABSTRACT

As the global transition away from fossil fuels accelerates, energy systems across the globe face a significant challenge. Given the high energy consumption of electric vehicle chargers, effective control is imperative to prevent local grid overload and congestion. In Uppsala, Sweden, a newly built parking garage includes 30 electric vehicle chargers, 62 kW solar energy production, and a 60 kW/137 kWh battery energy storage system. This paper presents a control algorithm that uses a negative correlation scheme, adjusted to the local grid load, to effectively manage the battery energy storage. To improve the performance of the algorithm, a genetic optimization method is applied to find the best feasible daily load profile for the parking garage. The results indicate that peak load and energy consumption during grid high-load hours can be significantly reduced. This also results in a 9.5 – 12.8 % reduction in electricity distribution fees at current prices as well as a peak load reduction of up to 50 %. Increasing the battery capacity and charging/discharging power in the scenarios analysed within the study will improve the algorithm's ability to achieve a satisfactory negative correlation between the load demand of the facility and the local grid. The proposed control algorithm lowers the facility's impact on the local grid during high-load peak hours by utilizing the battery energy storage system at the parking garage. Moreover, it decreases the distribution fees of the facility by lowering the load peaks and shifting the electricity consumption to the morning and night.

1. Introduction

The production, distribution, and transmission of electricity play an essential role in the advancement of modern society. To buy electricity, the electricity market has been formed and classified into two types: regulated and deregulated. The regulated electricity market can be described as a monopoly since the generation, distribution, and transmission of electricity are operated by the same company or party, and the individual consumer cannot choose where to purchase electricity. The deregulated electricity market instead splits the monopoly into sections so that many different parties can participate, creating a free and competitive market.

In the deregulated market, the price is set by the principle of supply and demand - producers of electricity bid on how much electricity they want to sell and for how much, and in turn, the retail electricity suppliers bid on how much electricity they want to buy [1]. The retail electricity suppliers, in turn, sell the electricity to the end-consumers such as households and companies. The process of the deregulated market is overseen and managed by the Swedish energy markets inspectorate (Ei) - who strive to create a robust, reliable, and

competitive market where the price of electricity is determined by the open market. Since a regulatory reform in 1996, Sweden has had a deregulated electricity market, and it is operated by the transmission system operator (TSO) Svenska Kraftnät [2].

As mentioned, the price of electricity is determined by the principle of supply and demand — meaning that if there are fluctuations in supplied electricity or in electricity demand, there might be fluctuations in the electricity price. The reason for this could be that there is not enough local electricity production in the area or that the production is affected by external factors, such as weather conditions. In such cases, electricity has to be imported from other areas or countries to meet the demand. Alternatively, services such as demand and energy flexibility can be utilized [3]. A more recent cause of electricity price fluctuations is the current war in Ukraine, which impacts the import of gas to Europe and, consequently, the price of electricity in Europe [4,5].

The amount of used electricity and the corresponding fees are expressed in a tariff, usually paid monthly. A common electricity tariff for companies in Sweden, with a subscription for more than 80 A, is the power tariff: A tariff that is determined by the total energy usage and

^{*} Corresponding author.

E-mail address: alexander.wallberg@angstrom.uu.se (A. Wallberg).

<https://doi.org/10.1016/j.apenergy.2024.124082>

Received 1 February 2024; Received in revised form 15 June 2024; Accepted 27 July 2024

Available online 9 August 2024

0306-2619/© 2024 The Author(s). Published by Elsevier Ltd. This is an open access article under the CC BY license (<http://creativecommons.org/licenses/by/4.0/>).

Abbreviation	
EV	Electric vehicle
BESS	Battery energy storage system
PV	Photovoltaic
PS	Population size
TC	Termination condition
SoC	State of charge
SoH	State of health
LF	Load factor
Ei	The Swedish energy markets inspectorate
TSO	Transmission system operator
DSO	Distribution system operator
GA	Genetic algorithm
NN	Neural network
PSO	Particle swarm optimization
Nomenclature	
ρ_p	Pearson correlation coefficient
P_{demand}	Load demand
P_{grid}	Grid load demand
P_{target}	Target load demand
FF	Fitness function
P_{BESS}	Charge/discharge power
P_{BESS}^{max}	Maximal charge/discharge power
$\epsilon_{monthly}^{peak}$	Highest monthly power fee
$\epsilon_{monthly}^{transfer}$	Total monthly transfer fee
$\epsilon_{transfer}^{t_{high}}$	Monthly transfer fee during t_{high}
$\epsilon_{transfer}^{t_{low}}$	Monthly transfer fee during t_{low}
$\epsilon_{monthly}^{tax}$	Monthly energy tax fee
$\epsilon_{monthly}^{distribution}$	Monthly distribution fee
$E_{monthly}$	Monthly transferred energy
E_{daily}	Daily transferred energy
$E_{daily}^{t_{high}}$	Daily transferred energy during t_{high}
$E_{daily}^{t_{low}}$	Daily transferred energy during t_{low}
$E_{monthly}^{t_{high}}$	Monthly transferred energy during t_{high}
$E_{monthly}^{t_{low}}$	Monthly transferred energy during t_{low}
E_{daily}^{peak}	Highest daily load peak
$E_{monthly}^{peak}$	Highest monthly load peak
t_{low}	Low peak time
t_{high}	High peak time

trading fee and monthly distribution fee ($\epsilon_{distribution}^{monthly}$). The trading fees include fees such as contracted energy, TSO fee, and certificates and are primarily based on the monthly total of transferred energy. On the other hand, $\epsilon_{distribution}^{monthly}$ primarily refer to fees based on factors such as the highest monthly power peak, at which time of the day the electricity is transferred to the facility, and fees associated with energy tax.

The $\epsilon_{peak}^{monthly}$ is determined by the highest monthly load peak in the P_{demand} of a facility. The monthly transfer fee during t_{high} ($\epsilon_{transfer}^{t_{high}}$) refers to the used electricity in the period: Monday–Friday 06:00–22:00 November to March, i.e., the daytime during the winter months, and the rest of the time is regarded as t_{low} . $\epsilon_{transfer}^{t_{high}}$ is generally 3–4 times higher than the monthly transfer fee during t_{low} ($\epsilon_{transfer}^{t_{low}}$), creating an economic incentive to shift as much energy as possible to the t_{low} , at least during November–March. It has been reported in previous research that the highest monthly peak can account for as much as 30% of the total monthly power subscription cost [7,8]. This indicates that reducing the highest peak during a given month would have a noticeable impact on the overall power subscription cost.

A common approach to reducing fees on a local level is to alter a facility's P_{demand} by installing a BESS and using it to perform peak shaving to reduce the highest power demand [9–12]. For facility owners, peak shaving can also postpone the expensive upgrades and allow for a reduction in the necessary power subscription. As the name suggests, the aim of peak shaving is to reduce the peaks of a facility's P_{demand} by utilizing stored electricity instead of electricity from the grid. A common way to evaluate the performance of the peak shaving is by calculating the LF of the P_{demand} [13,14]:

$$LF = \frac{P_{avg}}{P_{peak}} \tag{1}$$

where P_{avg} is the average power and P_{peak} is the highest peak. Typically, previously published peak shaving methods strive for economic benefits by reducing fees, given that the highest monthly peak impacts the customer's invoice. This is achieved by lowering the load peaks and aiming for $LF = 1$. However, the goal of these peak shaving methods can be derived in different ways. The common approaches can be classified into two categories:

(1) *Rule-based peak shaving.* The rule-based peak shaving methods operate by following a predetermined set of rules and if-then statements to reduce the load peaks in the P_{demand} [15–18]. The rules and if-then statements are based on historical P_{demand} data. Therefore, the rule-based peak shaving methods are considered more easily implemented and cannot generally generate optimized peak shaving strategies [18].

(2) *Optimization-based peak shaving.* The optimization-based peak shaving methods uses optimization techniques, such as neural network (NN), particle swarm optimization (PSO), and GA to find the most efficient way to reduce peak demand [19–23]. The chosen optimization method can take various factors into account such as P_{demand} , electricity price, and system constraints. Optimization algorithms adjust the peak shaving operation to minimize P_{demand} by striving to satisfy a specific objective, such as minimizing fees [24].

The traditional peak shaving methods aim at optimizing the electricity consumption by analysing a P_{demand} and local parameters such as BESS capacity. Therefore, these methods focus on local benefits such as reducing the power subscription fees, maximizing profit, and reducing the impact on the BESS state of health (SoH) and degradation [9,13,26–28]. However, by altering the local P_{demand} with such peak shaving, the system's impact on the local grid might contribute to grid congestion, i.e., the power peaks of the altered P_{demand} might overlap with the peaks on the grid as presented in Fig. 2. Overlapping local and grid peaks would contribute to grid congestion, which is not desired from a grid point of view [25,29].

Another perspective regarding peak shaving would instead be to utilize a local BESS as a peak shaving service for the distribution system operator (DSO) by alleviating the local grid instead of maximizing profit or reducing battery degradation [30]. One way of achieving

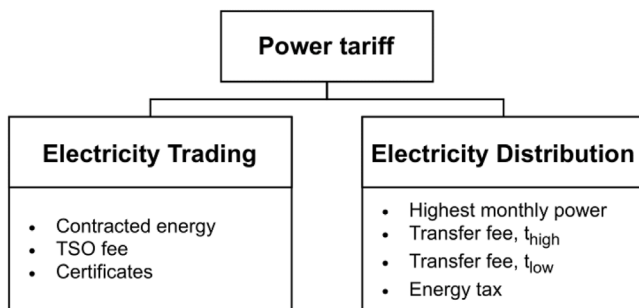


Fig. 1. Structure of the power tariff.

the highest load demand peak during a month [6]. As can be seen in Fig. 1, the power tariff can be divided into two primary fees: Monthly

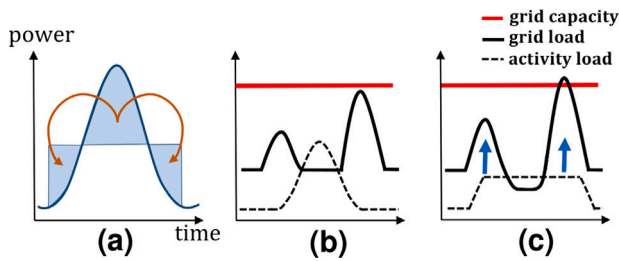


Fig. 2. The potential risks of implementing traditional peak shaving (LF = 1) without taking the grid into consideration. (a) Concept of peak shaving, (b) load demand of activity/facility and grid, and (c) potential risk of peak shaving contributing to grid congestion [25].

this could be for a facility to get P_{demand} to be negatively correlated with the P_{grid} . The facility that this study focuses on is the technical system of a parking garage called Dansmästaren, which is located in Uppsala, Sweden (See Fig. 3). The parking garage is equipped with 60 charging points, a 60 kW/137 kWh BESS, and 62 kW photovoltaic (PV) system [29,31]. The parking garage has a transformer rated for 345 kW and P_{demand} of the facility primarily consists of electricity for electric vehicle (EV) charging and some smaller loads such as lights, elevators, and ventilation. Previous research has been conducted on how to utilize the local BESS to lower Dansmästaren's power peaks by implementing a rule-based peak shaving method [32]. In the previous work, a neural network was constructed to predict the parking garage's P_{demand} , and thereafter, the predicted P_{demand} was used to create a peak shaving strategy. The ruled-based peak shaving method lowered the parking garage's P_{demand} by 25.4–38.5% which resulted in local benefit, i.e., monetary revenue. However, the grid load demand was not taken into consideration, and therefore, the facility's load demand might contribute to grid congestion, as shown in Fig. 2.

1.1. Scope of this paper

The paper presents a control method for a facility that aims to alter the P_{demand} by utilizing the local BESS. The desired P_{demand} should have perfect negative correlation (−1) with the local grid. While aiming to achieve perfect negative correlation, the resulting P_{demand} will also be evaluated by how much the load peak was reduced and how much energy was shifted from t_{high} to t_{low} . Thus, the work presented in this paper studies how a facility with a smart energy system can contribute to a wider system perspective – in this case to a municipality – by reducing the impact on a burdened grid, rather than prioritizing monetary revenue for the parking garage. The contributions of this paper are:

1. The article presents a novel optimized-based peak shaving method that contributes to counteracting and alleviating local grid congestion, while still providing monetary revenue for the owner of the facility. This is achieved by choosing correlation as a metric for comparison between the facility load profile and the grid load profile. Hence, correlation becomes an input variable for the proposed model. Additionally, the methodology described in the paper includes a new way of quantitatively evaluating the performance of the peak shaving method.
2. Data from a real facility is analysed. In particular, measurements from a commercial parking garage in Uppsala, Sweden, are used as inputs to the model. The data includes the facility's P_{demand} and system specifications, as well as the grid load demand. Furthermore, the paper presents what the capacity of the BESS should have been in worst-case scenarios to obtain a resulting P_{demand} with perfect negative correlation to the local grid profile.

Table 1
Input array for GA fitness function.

Input	Value	Initial value	Size
P_{target}	$[P_{target,1}, \dots, P_{target,24}]$	P_{demand}	24×1
$SoC_{initial}$	0 – 100%	50%	1×1

3. An economic evaluation based on the current electricity market is conducted, showing the impact of the proposed peak shaving during two worst-case scenarios, highlighting how much the load peaks were reduced and how much electricity was shifted from t_{high} to t_{low} .

2. Method

The aim of the control method presented in this paper was to provide a facility, like the parking garage at Dansmästaren, with an hour-by-hour control scheme that strives to alter P_{demand} (24 values [kWh/h] in consecutive order) to create a new load demand. This new load is referred to as P_{target} and should be negatively correlated to the local grid load. In this paper, Pearson correlation is used and the ρ_p ranges between −1 and +1. A positive ρ_p close to +1 indicates a positive relationship between the P_{demand} of the facility and P_{grid} during a given period, and a ρ_p close to −1 indicates the opposite. ρ_p close to 0, positive or negative, indicates that the curves are not related and behave independently of each other.

2.1. Model formulation

A genetic algorithm (GA) was programmed in MATLAB with the goal of finding a P_{target} , based on the parking garage's P_{demand} , with a perfect negative ρ_p to the local grid. GA is a heuristic search and optimization technique adept at finding near-optimal solutions using probabilistic selection rules and handling non-linear and complex problems. GA was chosen as the optimization technique because it aims at finding the global optimum, rather than getting stuck in any local optima, and because of its ability to evaluate solutions in parallel.

The GA operates as presented in Fig. 4, and the process is initiated by defining the FF. The function FF is used by the GA to find a desirable P_{target} . In this paper, the GA prioritized the search for a P_{target} that has a ρ_p close to −1. The P_{target} was produced by altering the P_{demand} of the parking garage by utilizing the local BESS. Therefore, the FF includes the ρ_p and load peak of the sought-after P_{target} in relation to the load peak in P_{demand} . The FF was defined as follows:

$$FF = (1 + \rho_p) + \frac{\max(P_{target})}{\max(P_{demand})}, \quad (2)$$

where ρ_p is the Pearson correlation coefficient of P_{target} and P_{grid} . As the goal of the GA is to find a suitable P_{target} by minimizing Eq. (2), the problem can be expressed as:

$$\min FF \quad (3)$$

The 25 inputs to the GA and their initial values are shown in Table 1 and the BESS parameters are shown in Table 2. Note that in the initialization of the GA, the P_{target} (24 values [kWh/h] in consecutive order) is set to P_{demand} and the initial SoC is set to 50%. $SoC_{initial}$ is the SoC of the BESS at the beginning of the day. P_{target} and $SoC_{initial}$ are then altered in the process as the GA searches for a solution as illustrated in Fig. 4 (see Table 2).

The GA was supplied with constraints to the model's inputs and parameters (See Table 3), such as constraints for the battery SoC and charge/discharge power (P_{BESS}) described by constraints C1 and C2. To create a realistic new load demand, the resulting P_{target} must also contain an equal amount of energy as the original P_{demand} as described by constraint C3. Finally, to assist the GA to find a P_{target} with a lower load peak than in the P_{demand} it was also given constraint C4.



Fig. 3. Mobility house Dansmästaren in Uppsala, Sweden. Cropped version of the figure presented in [32].

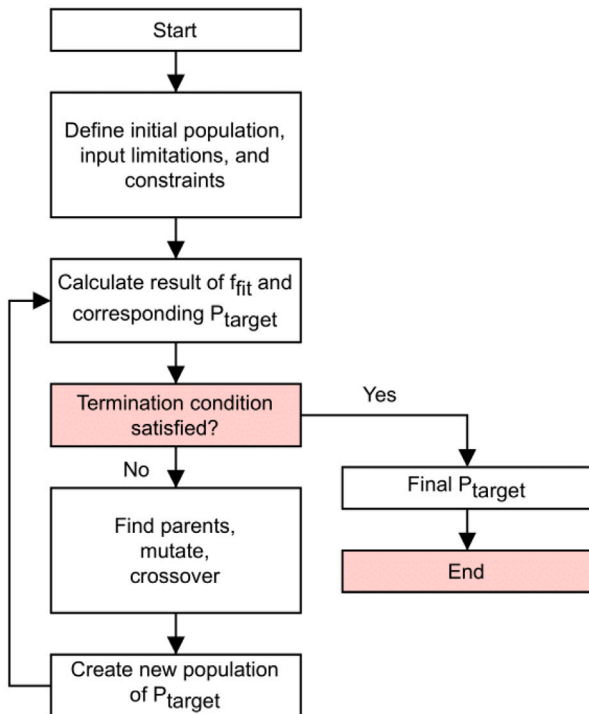


Fig. 4. Flow diagram of genetic algorithm.

At the end of a generation, the best P_{target} curves from the current population are defined by calculating their results of the FF. These P_{target} curves are considered parents for the next population and generation. However, before starting the next generation, the parents are altered by randomly changing some values in their sequence, called mutation, and by combining parents, called crossover, to create a new population. Thereafter, the next generation is started, and this process

Table 2
BESS parameters used in GA.

Variable	Value
SoC_{MIN}	0 kWh
SoC_{MAX}	137 kWh
P_{BESS}^{max}	60 kW

Table 3
GA constraints.

Constraint	Description
C1	$SoC_{MIN} \leq SoC \leq SoC_{MAX}$
C2	$0 \leq P_{BESS} \leq P_{BESS}^{max}$
C3	$\sum_{i=1}^{24} P_{demand} = \sum_{i=1}^{24} P_{target}$
C4	$0 \leq [P_{target,1}, \dots, P_{target,24}] \leq \max(P_{demand})$

is repeated until at least one termination condition (TC) is met (See Table 4). Once the process is terminated, the P_{target} that achieved the lowest ρ_p is selected to be used.

The first termination condition, TC1, was set to 0 due to the nature of Eq. (2). A FF result close to 0 indicates that a suitable P_{target} has been found since that would mean that ρ_p close to -1 and that the load peak of P_{target} has been lowered as much as possible. However, a fitness function result in the ranged [0 0.5] was also regarded as sufficient since that indicates that $\rho_p < -0.5$, i.e., close to -1 , and that the load peak of P_{target} was lower than the load peak of P_{demand} as can be seen in Fig. 5.

The population size (PS) of the GA was selected by performing a sensitivity analysis ranging from a PS of 10 to 2000. The second and third termination conditions, TC2 and TC3, were arbitrarily selected to 50 and 10. The GA found a suitable solution when the PS ≥ 250 on D_1 and PS ≥ 1000 on D_2 . Therefore, a population size of 1000 was selected for the GA. The sensitivity analysis can be found in the supplementary material.

2.2. Data collection and handling

The presented method was created and tested using data collected from the technical systems at the parking garage at Dansmästaren. The installed 60 kW/137 kWh BESS used in the proposed control method

Table 4

The termination conditions for the GA.

Termination condition	Value	Description
TC1 - Fitness Limit	0	The GA terminates if the result of the FF is less than the Fitness Limit.
TC2 - Max Generations	50	The maximum number of generations that the GA is allowed to execute before terminating.
TC3 - Max Stall Generations	10	The number of generations the GA is allowed to stall before terminating.

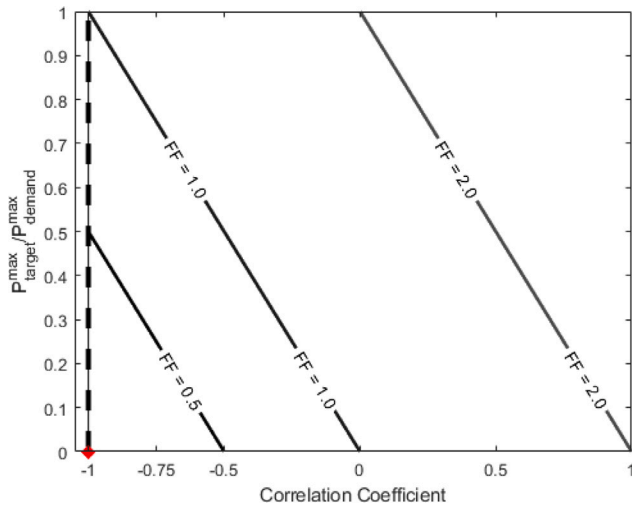


Fig. 5. All possible fitness function results with input $-1 \leq \rho_p \leq 1$ and $0 \leq P_{target}^{max} / P_{demand}^{max} \leq 1$. The dashed line on the left side shows all FF solutions with perfect negative correlation and the red diamond, \blacklozenge , is the solution the GA strives for.

was the same as presented in previously published work [31,32]. The parking garage's P_{demand} data used in the presented control method were obtained from the technical systems at Dansmästaren and have an hourly resolution (kWh/h). P_{grid} data was obtained from the Swedish TSO Svenska Kraftnät with an hourly resolution (MWh/h). Information regarding the payments and invoices from the parking garage was obtained from the DSOs, Vattenfall, customer portal. Based on the invoice data from the parking garage from 2021, $\epsilon_{peak}^{monthly}$ accounted for approximately 20% of the total electricity distribution fees. Further based on the same invoice data, $\epsilon_{transfer}^{high}$ was 0.48 SEK/kWh, $\epsilon_{transfer}^{low}$ was 0.144 SEK/kWh, and ϵ_{peak} was 37 SEK/kWh.

The highest load peaks at Dansmästaren typically occur during the winter months (January–March and November–December) and the risk for congestion in the grid is higher during the same period of the year. As a consequence of this, the price of electricity is higher in the winter and therefore also the need for energy management. Two days within that period were selected to test the performance of the proposed peak shaving: December 7 and November 28. On November 28, 2021, Dansmästaren experienced the highest peak load demand, while the grid had its highest peak load demand on December 7, 2021. These two days were, therefore, declared as the two worst-case scenarios in regard to grid congestion and used to investigate how the presented peak shaving method would operate under such conditions. The selected days and their respective ρ_p between P_{demand} and the grid can be seen in Table 5. The load demand at Dansmästaren and the grid during the two selected days are shown in Fig. 6 and 7.

The first day, D_1 , was selected for the purpose of testing and evaluating the peak shaving model during the day with the highest load peak on the local grid in 2021, which was on the 7th of December, with a grid load peak of 243.3 MWh/h. P_{grid} and P_{demand} of the parking garage during D_1 are shown in Fig. 6 and the ρ_p between the two load demands was 0.2637.

Table 5

The two days used to test the performance of the proposed peak shaving method as well as their respective ρ_p to the grid before implementing peak shaving.

Day	Description	ρ_p
D_1	The day when P_{grid} had the highest load peak during the winter months	0.2637
D_2	The day when P_{demand} had the highest load peak during the winter months	0.2549

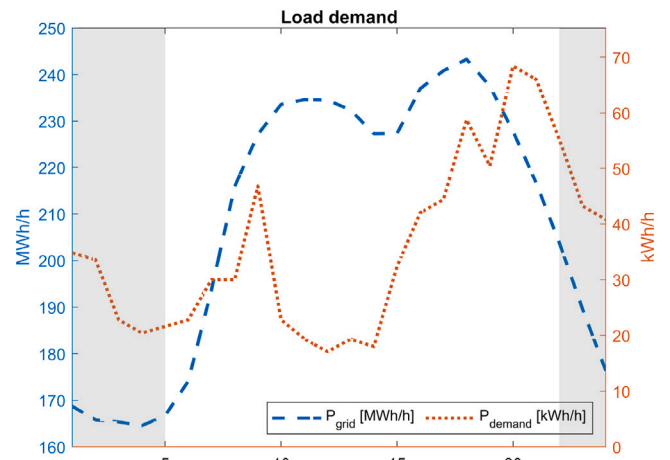


Fig. 6. D_1 , December 7, 2021. P_{grid} and P_{demand} at Dansmästaren. Grey regions indicate t_{low} and white region corresponds to t_{high} .

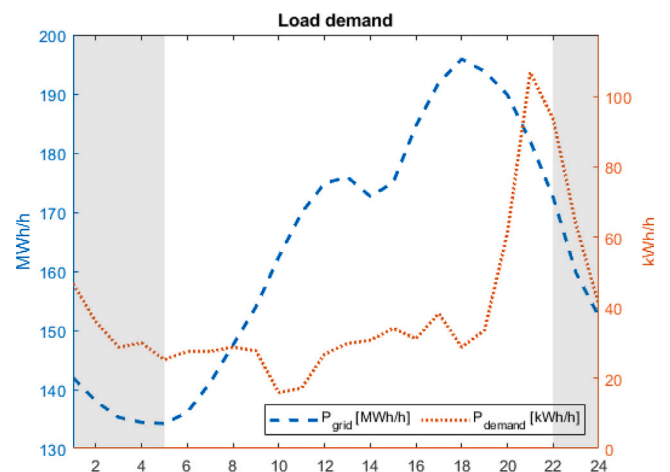


Fig. 7. D_2 , November 28, 2021. P_{grid} and P_{demand} at Dansmästaren. Grey regions indicate t_{low} and white region corresponds to t_{high} .

The second day, D_2 , used for the model was the day with the highest load peak at the parking garage, which was the 28th of November 2021, with a load peak of 106.8 kWh/h. The P_{grid} and the P_{demand} of the parking garage during D_2 are shown in Fig. 7 and the ρ_p between the two load demands was 0.2549.

Table 6

Correlation coefficient, load peak and energy used during t_{low} and t_{high} for P_{demand} and P_{target} in day D_1 at Dansmästaren.

	P_{demand}	P_{target}	ΔkWh
ρ_p	0.26	-0.86	-
E_{peak}^{daily}	68.4 kWh	47.0 kWh	21.4 kWh
$E_{t_{low}}^{daily}$	217.2 kWh	324.7 kWh	107.5 kWh
$E_{t_{high}}^{daily}$	634.8 kWh	537.1 kWh	

The ρ_p of the two presented days indicate a positive relationship between P_{demand} and P_{grid} , although it was not particularly strong. Nevertheless, as can be seen in Figs. 6 and 7, there was a moderate overlap between the load peaks at the parking garage and the local grid.

3. Result & discussion

To evaluate the performance of the GA and the resulting P_{target} , the final correlation to the grid was used. Additionally, two other factors were taken into consideration: How low the load peak in P_{target} was compared to in P_{demand} , and how much energy was shifted from t_{high} to t_{low} in the selected days. These two factors were then used to calculate the monetary benefits of the implementation of the proposed peak shaving method.

3.1. Target load demand

The proposed control was implemented on D_1 and D_2 . The resulting P_{target} compared to P_{demand} and P_{grid} , as well as the SoC cycle of BESS are shown in Figs. 8 and 10. The P_{demand} of “traditional” peak shaving (Trad) with $LF = 1$ is also presented in the figures as a baseline for comparison.

During D_1 , ρ_p improved from 0.26 to -0.86 (Table 6) and the resulting P_{target} can be seen in Fig. 8. The initial P_{demand} of the parking garage consisted of a total of 861.0 kWh on D_1 , i.e., daily transferred energy (E_{daily}) was 861.0 kWh. Out of E_{daily} on D_1 , 25.2% of the energy transfer occurred during t_{low} meaning that daily transferred energy during t_{low} ($E_{t_{low}}^{daily}$) = 217.2 kWh and 74.8% occurred during t_{high} meaning that daily transferred energy during t_{high} ($E_{t_{high}}^{daily}$) was 634.8 kWh.

However, after the proposed peak shaving control was implemented $E_{t_{low}}^{daily}$ increased to 324.7 kWh which corresponds to 37.7% of E_{daily} on D_1 . At the same time, $E_{t_{high}}^{daily}$ decreased to 537.1 kWh which corresponds to 62.3% of E_{daily} . In other words, 12.5 percentage points of E_{daily} was shifted from t_{high} to t_{low} .

The $\epsilon_{transfer}^{monthly}$ including the contribution of both the $\epsilon_{transfer}^{t_{high}}$ and the $\epsilon_{transfer}^{t_{low}}$, is calculated as shown in Eq. (4).

$$\epsilon_{transfer}^{monthly} = E_{t_{high}}^{monthly} \times \epsilon_{transfer}^{t_{high}} + E_{t_{low}}^{monthly} \times \epsilon_{transfer}^{t_{low}} \quad (4)$$

In December 2021, the month when D_1 occurred, the monthly transferred energy ($E_{monthly}$) was 25 312 kWh. Out of the total, the monthly transferred energy during t_{high} ($E_{t_{high}}^{monthly}$) was 12 850 kWh which corresponds to 50.8% and monthly transferred energy during t_{low} ($E_{t_{low}}^{monthly}$) was 12 462 kWh which in turn corresponds to 49.2%. At Dansmästaren, $\epsilon_{transfer}^{t_{high}}$ was 0.48 SEK/kWh and $\epsilon_{transfer}^{t_{low}}$ was 0.144 SEK/kWh in 2021. Using Eq. (4) before applying the proposed peak shaving the resulting $\epsilon_{transfer}^{monthly}$ was 7962.5 SEK. However, assuming that the shifting of energy from t_{high} to t_{low} is the same on a monthly basis, 12.5 percentage points, $E_{t_{high}}^{monthly}$ decreases to 9694.5 kWh, i.e., 38.3% of $E_{monthly}$. At the same time, $E_{t_{low}}^{monthly}$ increases to 15 618 kWh, i.e., 61.7% of $E_{monthly}$. Using Eq. (4) after applying the proposed peak shaving the resulting $\epsilon_{transfer}^{monthly}$ became 6902.4 SEK, resulting in a 13.3% reduction of the $\epsilon_{transfer}^{monthly}$

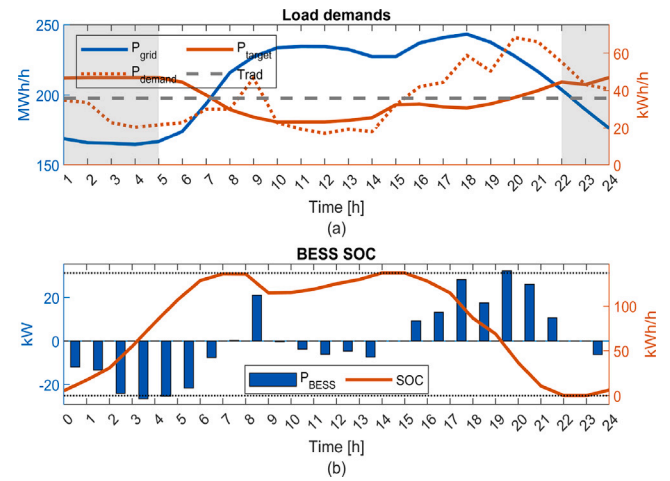


Fig. 8. D_1 , December 7, 2021. (a) Resulting P_{target} alongside P_{demand} and P_{grid} as well as (b) BESS SoC. Grey regions indicate t_{low} and white region corresponds to t_{high} .

Table 7

Distribution fees at Dansmästaren: $\epsilon_{peak}^{monthly}$, $\epsilon_{transfer}^{monthly}$, $\epsilon_{distribution}^{monthly}$ for D_1 at Dansmästaren for P_{demand} and P_{target} as well as the reduction.

	P_{demand}	P_{target}	ΔSEK
$\epsilon_{peak}^{monthly}$	2530.8 SEK	1739.0 SEK	791.8 SEK
$\epsilon_{transfer}^{monthly}$	7962.5 SEK	6902.4 SEK	1060.1 SEK
$\epsilon_{distribution}^{monthly}$	9011.1 SEK	9011.1 SEK	0 SEK
$\epsilon_{distribution}^{monthly}$	19 504.4 SEK	17 652.5 SEK	1851.9 SEK

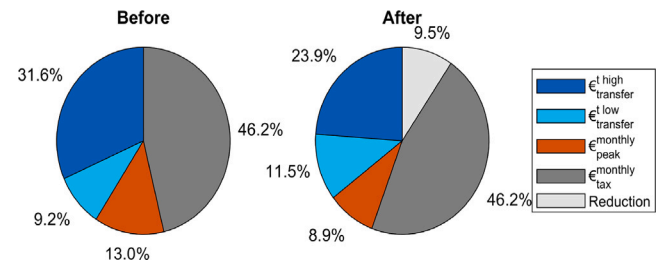


Fig. 9. Distribution fee on D_1 before and after implementing negative correlation peak shaving control.

Additionally, the highest daily load peak (E_{peak}^{daily}) on D_1 decreased from 68.4 kWh to 47.0 kWh, i.e., reducing $\epsilon_{peak}^{monthly}$ from 2530.8 SEK to 1739.0 SEK. The final part of the distribution fees, monthly energy tax fee ($\epsilon_{tax}^{monthly}$) is 0.356 SEK/kWh and is based on the $E_{monthly}$ which is not affected by the peak shaving operation. Therefore, $\epsilon_{tax}^{monthly}$ is the same before and after applying the proposed peak shaving. $\epsilon_{distribution}^{monthly}$ for a given month is calculated using Eq. (5).

$$\epsilon_{distribution}^{monthly} = \epsilon_{peak}^{monthly} + \epsilon_{transfer}^{monthly} + \epsilon_{tax}^{monthly} \quad (5)$$

The contribution of each type of fee in the distribution fee before (P_{demand}) and after (P_{target}) applying the proposed peak shaving can be seen in Table 7.

Combining the contribution from the reduction in $\epsilon_{peak}^{monthly}$ and $\epsilon_{transfer}^{monthly}$ during December 2021 was reduced from 19 504.4 SEK to 17 652.5 SEK, i.e., a reduction of 9.5%. The impact on $\epsilon_{distribution}^{monthly}$ in the total electricity distribution fee in D_1 can be seen in Fig. 9.

During D_2 , ρ_p improved from 0.25 to -0.54 (Table 8) and the resulting P_{target} can be seen in Fig. 10. On D_2 E_{daily} was 931.2 kWh, and during that day, the parking garage had its highest load peak at Dansmästaren in 2021, i.e., $E_{peak}^{daily} = 106.8$ kWh. On D_2 29.1% of

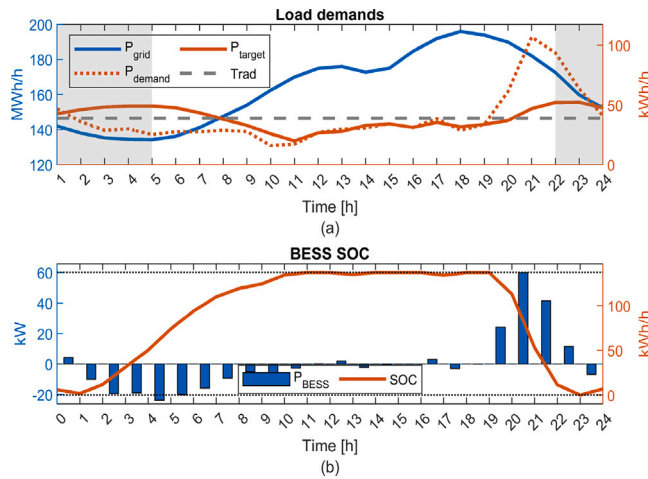


Fig. 10. D_2 , November 28, 2021. (a) Resulting P_{target} alongside P_{demand} and P_{grid} as well as (b) BESS SoC. Grey regions indicate t_{low} and white region corresponds to t_{high} .

Table 8

Correlation coefficient, load peak and energy used during t_{low} and t_{high} for P_{demand} and P_{target} in day D_2 at Dansmästaren.

	P_{demand}	P_{target}	ΔkWh
ρ_p	0.25	-0.54	-
E_{peak}^{daily}	106.8 kWh	52.2 kWh	54.6 kWh
$E_{t_{low}}^{daily}$	271.2 kWh	334.7 kWh	57.2 kWh
$E_{t_{high}}^{daily}$	660.0 kWh	596.5 kWh	-

E_{daily} occurred during t_{low} , i.e., $E_{t_{low}}^{daily} = 271.2$ kWh. Therefore during the same day, $E_{t_{high}}^{daily} = 660.0$ kWh, i.e., 70.9% of E_{daily} . However, after the proposed peak shaving control was implemented, the amount of energy during t_{low} increased to 334.7 kWh (35.9%) and decreased to 596.5 kWh (64.1%) during t_{high} . In other words, 6.8 percentage points of the energy was shifted from t_{high} to t_{low} .

In November 2021, the month when D_2 occurred, the $E_{monthly}$ was 22 785 kWh. Out of the total, the $E_{monthly}^{t_{high}}$ was 12 103 kWh which corresponds to 53.1% and $E_{monthly}^{t_{low}}$ was 10 682 kWh which in turn corresponds to 46.9%. Using Eq. (4) before applying the proposed peak shaving the resulting $\epsilon_{transfer}^{monthly}$ was 7347.6 SEK. However, assuming that the shifting of energy from t_{high} to t_{low} is the same on a monthly basis, 6.1 percentage points, $E_{monthly}^{t_{high}}$ decreases to 10 709 kWh, i.e., 47% of $E_{monthly}$. At the same time, $E_{monthly}^{t_{low}}$ increases to 12 076 kWh, i.e., 53% of $E_{monthly}$. Using Eq. (4) after applying the proposed peak shaving the resulting $\epsilon_{transfer}^{monthly}$ became 6879.2 SEK, resulting in a 6.4% reduction of the $\epsilon_{transfer}^{monthly}$. Additionally, E_{peak}^{daily} decreased from 106.8 kWh to 52.2 kWh, hence, a reduction of 51.1%. Since $\epsilon_{peak}^{monthly}$ at Dansmästaren is calculated based on a fixed cost per kWh, $\epsilon_{peak}^{monthly}$ was reduced from 3951.6 SEK to 1931.4 SEK. The final part of the distribution fee, $\epsilon_{tax}^{monthly}$ is 0.356 SEK/kWh and is based on the $E_{monthly}$ which is not affected by the peak shaving operation. Therefore, $\epsilon_{tax}^{monthly}$ is the same before and after applying the proposed peak shaving. $\epsilon_{distribution}^{monthly}$ for a given month is calculated using Eq. (5).

The contribution of each type of fee in the distribution fees before (P_{target}) and after (P_{target}) applying the proposed peak shaving can be seen in Table 9.

Combining the contribution from the reduction in $\epsilon_{peak}^{monthly}$ and $\epsilon_{distribution}^{monthly}$, $\epsilon_{transfer}^{monthly}$ during November 2021 was reduced from 19 410.7 SEK to 16 922.1 SEK, i.e., a reduction of 12.8%. The impact on $\epsilon_{distribution}^{monthly}$ in the total electricity distribution fee in D_2 can be seen in Fig. 11.

Table 9

Distribution fees at Dansmästaren: $\epsilon_{peak}^{monthly}$, $\epsilon_{transfer}^{monthly}$, $\epsilon_{tax}^{monthly}$ for D_2 at Dansmästaren for P_{demand} and P_{target} as well as the reduction.

	P_{demand}	P_{target}	ΔSEK
$\epsilon_{peak}^{monthly}$	3951.6 SEK	1931.4 SEK	2020.2 SEK
$\epsilon_{transfer}^{monthly}$	7347.6 SEK	6879.2 SEK	468.4 SEK
$\epsilon_{tax}^{monthly}$	8111.5 SEK	8111.5 SEK	0 SEK
$\epsilon_{distribution}^{monthly}$	19 410.7 SEK	16 922.1 SEK	2488.6 SEK

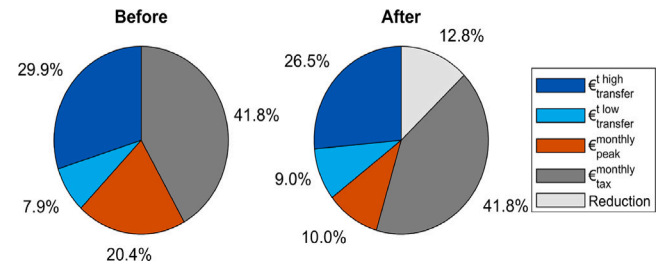


Fig. 11. Distribution fee on D_2 before and after implementing negative correlation peak shaving control.

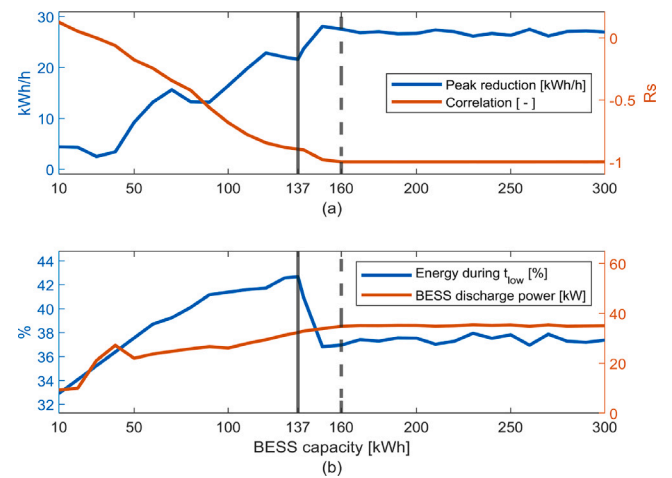


Fig. 12. D_1 , (a) Improvements in correlation and peak reduction and (b) amount of shifted energy as the battery capacity was increased from 0 to 300 kWh in 10 kWh increments. The grey vertical line shows ρ_p and the peak reduction using the current BESS capacity of 137 kWh and the dashed grey line show the necessary BESS capacity to obtain perfect negative correlation (-1).

3.2. Battery capacity optimization

As shown in Tables 6 and 8, the proposed peak shaving method was capable of altering the P_{demand} of the parking garage at Dansmästaren to improve ρ_p by making it more negative on the selected days. However, the current technical system was not dimensioned to achieve perfect negative correlation (-1).

In the case of D_1 and D_2 at Dansmästaren, P_{BESS} only reaches the P_{BESS}^{max} once (on D_2 between 20:00 and 21:00) as can be seen in Figs. 8b and 10b, indicating that P_{BESS}^{max} of 60 kW did affect the GA's ability to achieve perfect negative correlation. The local PV production did not impact the GA since the selected days occurred in the winter, i.e., a period when the PV production can be regarded as negligible. However, as Figs. 8b and 10b also show, the SoC of the BESS reaches 100% at some point during both days. When the BESS reaches 100% SoC, the system loses the ability to increase P_{demand} , i.e., the GA can no longer create a P_{target} with a higher value than P_{demand} since it cannot charge the BESS. The GA was limited to only discharging the BESS, and this has a direct impact on how close to -1 the resulting ρ_p can be. An

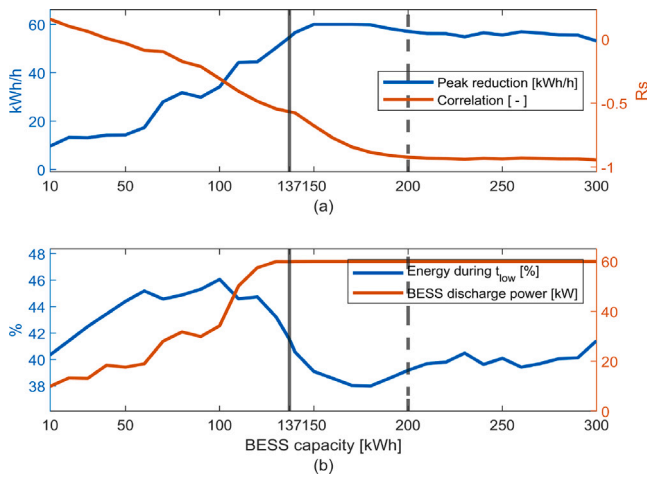


Fig. 13. D_2 , (a) Improvements in correlation and peak reduction and (b) amount of shifted energy as the battery capacity was increased from 0 to 300 kWh in 10 kWh increments. The grey vertical line shows ρ_p and the peak reduction using the current BESS capacity of 137 kWh and the dashed grey line shows the necessary BESS capacity to obtain perfect negative correlation on D_2 .

example of the model's inability to improve ρ_p , in the case when the BESS was fully charged, can be seen in Fig. 10a from 10:00 until 16:00. To reduce ρ_p further, the maximum capacity and P_{BESS}^{max} of the BESS would therefore need to be increased.

To investigate the required BESS capacity, the performance of peak shaving control using different maximum battery capacities (10–300 kWh) was simulated for D_1 and D_2 . The case of D_1 can be seen in Fig. 12 where the BESS capacity increased by 10 kWh at each iteration. For each step of BESS capacity, the model's ability to reduce the load peak, the correlation coefficient, the required P_{BESS} , and the amount of shifted energy are shown. As BESS capacity increases, the correlation improves until perfect negative correlation was achieved at approximately 160 kWh. At the same time, the improvements in peak reduction halt and reach a plateau, indicating that 160 kWh would be a suitable battery capacity on D_1 . Additionally, as can be seen in Fig. 12, the maximum required P_{BESS}^{max} was 35 kW, i.e., less than P_{BESS}^{max} . As can also be seen in the figure, the amount of shifted energy decreases when the BESS capacity ≥ 150 kWh. The shifting of energy from t_{high} to t_{low} generates less monetary revenue than lowering the load peak. For this reason, the reduction in shifted energy does not impact the resulting monetary benefits.

On D_2 the correlation stopped improving when the battery capacity increased to approximately 200 kWh. Similarly to D_1 , the peak reduction reached a plateau at the same time as the best correlation was achieved, and the amount of shifted time was also reduced as the correlation improved, as illustrated in Fig. 13b. The reason for the reduction in shifted energy was that the daily load peak on D_2 occurred between 19:00 and 24:00, as can be seen in Fig. 10, i.e., a part of the load peak already occurred during t_{low} . However, since the GA strives to lower the peak load demand rather than shifting the energy usage, an increasing part of the daily load peak was moved to t_{high} as the BESS capacity increased.

Increasing the battery capacity improves the GA's ability to achieve perfect negative correlation to the grid, as well as its ability to lower the load peaks. However as can be seen in Fig. 13, the P_{BESS}^{max} of 60 kW was limiting the GA's ability to achieve perfect negative correlation starting from a BESS capacity of approximately 130 kWh on D_2 . In order to rectify this, the P_{BESS}^{max} would need to be increased.

By removing the constraint C2, i.e., not restricting the GA with a maximum charge/discharge power of 60 kW, the GA was able to find a solution with perfect negative correlation with a BESS capacity of 190 kWh and P_{BESS}^{max} to 70 kW, as can be seen in Fig. 14. Therefore, unlike

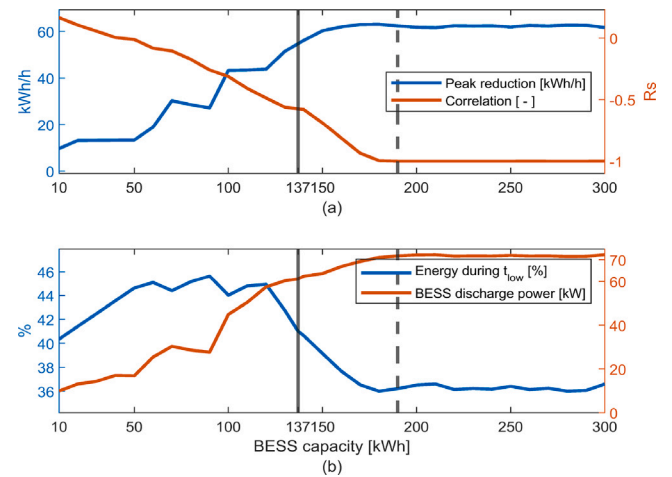


Fig. 14. D_2 , (a) Improvements in correlation and peak reduction and (b) amount of shifted energy as the battery capacity was increased from 0 to 300 kWh in 10 kWh increments without constraint C2, i.e., removing P_{BESS}^{max} . The grey vertical line shows ρ_p and the peak reduction using the current BESS capacity of 137 kWh and the dashed grey line shows the necessary BESS capacity to obtain perfect negative correlation on D_2 .

on D_1 , both the BESS capacity and the P_{BESS}^{max} had to be increased in order for the GA to find a P_{target} with perfect negative correlation.

As mentioned before, the GA chooses the initial SoC and, on both presented days, selected a low initial value for SoC. In D_1 and D_2 , the best solution found by the GA had initial SoC of 5.0% and 5.9% respectively as can be seen in Figs. 8 and 10. Additionally, the final SoC of the BESS on D_1 and D_2 reached 6.0% and 6.8% respectively. On both days, the final SoC ended up rather close to the initial SoC. The reason for this was due to constraint C4 and the overall daily profile of the local P_{grid} , specifically due to P_{grid} having its peaks in the middle the day and valleys at night and in the morning. Since the GA prefers to start the day at a low SoC in order to be able to achieve a ρ_p close to -1 , it was beneficial that it also preferred to end the day at a low SoC. This means that if the control strategy would be implemented on several sequential days at the parking garage, the initial SoC of the BESS of each day would be set to an appropriate value the day before.

To compare the optimization procedure on the two selected days, the resulting FF for the tested BESS capacities alongside the obtained ρ_p and load peak reduction can be seen in Fig. 15. On both days, the FF starts in the region $FF = 2$, and as the BESS capacity was increased ends up close to $FF = 0.5$.

Implementing the presented negative correlation peak shaving method in a facility such as Dansmästaren would lower the facility's contribution to grid congestion in the city. However, for the method to function in practice, one would need to implement a prediction model for the P_{demand} and P_{grid} since they are needed to find a peak shaving schedule.

4. Conclusion

Utilizing the local 60 kW/137 kWh BESS at the parking garage at Dansmästaren, the proposed peak shaving method was able to alter the P_{demand} to achieve negative correlation to the local grid and, at the same time, reduce the highest load peak. The advantage of the proposed method was that the resulting load demand generated both grid and local benefits by helping to alleviate grid congestion and lowering the transfer fees in the facility's electricity invoice. To achieve perfect negative correlation during the selected days, the BESS capacity would need to increase from 137 kWh to 160 kWh for D_1 and to 190 kWh for D_2 , and the charge and discharge power of BESS needed to be increased on D_2 , from 60 kW to 70 kW.

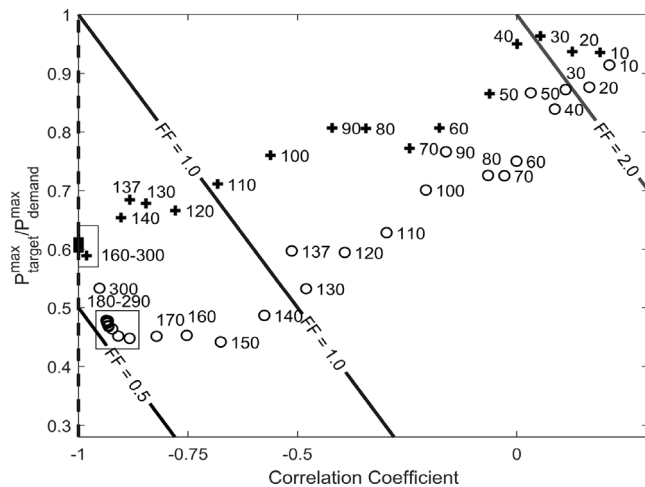


Fig. 15. Result of the FF as the BESS increased by 10 kWh increments for D_1 (+) and D_2 (o).

As illustrated in the results, even though the proposed peak shaving method primarily aims at reducing grid congestion by striving for negative correlation, it can still generate monetary revenue by reducing the load peaks and by shifting energy usage. Implementing this type of peak shaving control at a facility like Dansmästaren would help to counteract the grid congestion that the city of Uppsala is experiencing. In other words, the correlation between the load demand of a facility and the grid could be used as a quantitative way of evaluating the non-monetary benefits of peak shaving control. However, it is important to keep in mind that – to make a noticeable impact on a high-system level – multiple facilities would need to implement the proposed peak shaving control. This kind of control being implemented on a larger scale, e.g., in a city like Uppsala with multiple mobility houses, would reform how distributed generation works and assist the electrification of society and the transport sector.

CRediT authorship contribution statement

Alexander Wallberg: Writing – original draft, Visualization, Software, Methodology, Investigation, Conceptualization. **Valeria Castellucci:** Writing – review & editing, Supervision, Project administration, Conceptualization. **Carl Flygare:** Writing – review & editing, Visualization, Conceptualization. **Emil Lind:** Writing – review & editing. **Egil Schultz:** Writing – review & editing. **Marina Martins Mattos:** Writing – review & editing. **Rafael Waters:** Writing – review & editing, Supervision, Funding acquisition, Conceptualization.

Declaration of competing interest

The authors declare the following financial interests/personal relationships which may be considered as potential competing interests: Alexander Wallberg reports financial support was provided by Uppsala University. If there are other authors, they declare that they have no known competing financial interests or personal relationships that could have appeared to influence the work reported in this paper.

Data availability

Data will be made available on request.

Acknowledgements

The presented research was carried out in collaboration with the municipality-owned company Uppsala Parkerings AB, and the

foundation STUNS Energi. The research was funded by the Swedish Energy Agency, Sweden project 2019-03066. This work was also funded through the SweGRIDS, Sweden project FPS24, the Swedish Electromobility Centre, Sweden, STandUP for Energy by the Swedish Energy Agency, Sweden (Energimyndigheten), and the Swedish DSO Vattenfall, Sweden.

Appendix A. Supplementary data

Supplementary material related to this article can be found online at <https://doi.org/10.1016/j.apenergy.2024.124082>.

References

- [1] Kraftnät S. Hur hänger elpriser, elområden och kapacitetsavgifter ihop?. 2022, <https://www.svk.se/press-och-nyheter/nyheter/allmanna-nyheter/2022/hur-hanger-elpriser-elomraden-och-kapacitetsavgifter-ihop/>, [Accessed 05 May 2023].
- [2] energimarknadsbyrå K. Elmarknaden i sverige. 2020, <https://www.energi-marknadsbyran.se/el/elmarknaden/elmarknaden-i-sverige/>, [Accessed 06 June 2023].
- [3] Jensen SØ, Marszal-Pomianowska A, Lollini R, Pasut W, Knotzer A, Engelmann P, Stafford A, Reynnders G. IEA EBC annex 67 energy flexible buildings. Energy Build 2017;155:25–34. <http://dx.doi.org/10.1016/j.enbuild.2017.08.044>.
- [4] Ferriani F, Gazzani AG. The impact of the war in Ukraine on energy prices: Consequences for firms' financial performance. SSRN Electron J 2022;174(May):221–30. <http://dx.doi.org/10.2139/ssrn.4216406>.
- [5] Bella GD, Flanagan MMJ, Foda K, Maslova S, Pienkowski A, Stuermer M, Frederik M, Toscani G. Natural Gas in Europe: The Potential Impact of Disruptions to Supply. International Monetary Fund; 2022, no. July, <https://www.elibrary.imf.org/view/journals/001/2022/145/article-A001-en.xml>, WP/22/145.
- [6] A.B. VE. Elnätspriser och avtalsvillkor för företag. 2023, <https://www.svk.se/press-och-nyheter/nyheter/allmanna-nyheter/2022/hur-hanger-elpriser-elomraden-och-kapacitetsavgifter-ihop/>, [Accessed 05 May 2023].
- [7] Chua KH, Lim YS, Morris S. A novel fuzzy control algorithm for reducing the peak demands using energy storage system. Energy 2017;122:265–73. <http://dx.doi.org/10.1016/j.energy.2017.01.063>.
- [8] Sun Y, Wang S, Xiao F, Gao D. Peak load shifting control using different cold thermal energy storage facilities in commercial buildings: A review. Energy Convers Manage 2013;71:101–14. <http://dx.doi.org/10.1016/j.enconman.2013.03.026>.
- [9] Levron Y, Shmilovitz D. Power systems' optimal peak-shaving applying secondary storage. Electr Power Syst Res 2012;89:80–4. <http://dx.doi.org/10.1016/j.epr.2012.02.007>.
- [10] Chapaloglou S, Nesiadis A, Iliadis P, Atsonios K, Nikolopoulos N, Grammelis P, Yiakopoulos C, Antoniadis I, Kakaras E. Smart energy management algorithm for load smoothing and peak shaving based on load forecasting of an island's power system. Appl Energy 2019;238:627–42. <http://dx.doi.org/10.1016/j.apenergy.2019.01.102>.
- [11] Liu D, Jin Z, Chen H, Cao H, Yuan Y, Fan Y, Song Y. Peak shaving and frequency regulation coordinated output optimization based on improving economy of energy storage. Electronics (Switzerland) 2022;11(1). <http://dx.doi.org/10.3390/electronics11010029>.
- [12] Chua KH, Lim YS, Morris S. Peak reduction for commercial buildings using energy storage. In: IOP Conference Series: Earth and Environmental Science. Vol. 93, 2017, <http://dx.doi.org/10.1088/1755-1315/93/1/012008>.
- [13] Rana MM, Atef M, Sarkar MR, Uddin M, Shafiullah GM. A review on peak load shaving in microgrid—Potential benefits, challenges, and future trend. Energies 2022;15(6):1–17. <http://dx.doi.org/10.3390/en15062278>.
- [14] Uddin M, Romlie MF, Abdullah MF, Halim SA, Halim A, Bakar A, Chia T. A review on peak load shaving strategies. Renew Sustain Energy Rev 2018;82(November 2017):3323–32. <http://dx.doi.org/10.1016/j.rser.2017.10.056>.
- [15] Manojkumar R, Kumar C, Ganguly S, Gooi HB, Mekhilef S, Catalao JP. Rule-based peak shaving using master-slave level optimization in a diesel generator supplied microgrid. IEEE Trans Power Syst 2023;38(3):2177–88. <http://dx.doi.org/10.1109/TPWRS.2022.3187069>.
- [16] Guo Y, Zhang Q, Wang Z. Cooperative peak shaving and voltage regulation in unbalanced distribution feeders. IEEE Trans Power Syst 2021;36(6):5235–44. <http://dx.doi.org/10.1109/TPWRS.2021.3069781>.
- [17] Zhou B, Xu D, Chan KW, Li C, Cao Y, Bu S. A two-stage framework for multi-objective energy management in distribution networks with a high penetration of wind energy. Energy 2017;135:754–66. <http://dx.doi.org/10.1016/j.energy.2017.06.178>.
- [18] Abbasi A, Khalid HA, Rehman H, Khan AU. A novel dynamic load scheduling and peak shaving control scheme in community home energy management system based microgrids. IEEE Access 2023;11(February):32508–22. <http://dx.doi.org/10.1109/ACCESS.2023.3255542>.

- [19] Li X, Cao X, Li C, Yang B, Cong M, Chen D. A coordinated peak shaving strategy using neural network for discretely adjustable energy-intensive load and battery energy storage. *IEEE Access* 2020;8:5331–8. <http://dx.doi.org/10.1109/ACCESS.2019.2962814>.
- [20] Mahmud K, Sahoo A. Multistage energy management system using autoregressive moving average and artificial neural network for day-ahead peak shaving. *Electron Lett* 2019;55(15):853–5. <http://dx.doi.org/10.1049/el.2019.0890>.
- [21] Zhu F, an Zhong P, Xu B, Liu W, Wang W, Sun Y, Chen J, Li J. Short-term stochastic optimization of a hydro-wind-photovoltaic hybrid system under multiple uncertainties. *Energy Convers Manage* 2020;214(1):112902. <http://dx.doi.org/10.1016/j.enconman.2020.112902>.
- [22] Kalkhambkar V, Kumar R, Bhakar R. Energy loss minimization through peak shaving using energy storage. *Perspect Sci* 2016;8:162–5. <http://dx.doi.org/10.1016/j.pisc.2016.04.022>.
- [23] Ghafoori M, Abdallah M, Kim S. Electricity peak shaving for commercial buildings using machine learning and vehicle to building (V2B) system. *Appl Energy* 2023;340(November 2022):121052. <http://dx.doi.org/10.1016/j.apenergy.2023.121052>.
- [24] Mahmud K, Hossain MJ, Town GE. Peak-load reduction by coordinated response of photovoltaics, battery storage, and electric vehicles. *IEEE Access* 2018;6:29353–65. <http://dx.doi.org/10.1109/ACCESS.2018.2837144>.
- [25] Flygare C, Wallberg A, Jonasson E, Castellucci V, Waters R. Correlation as a method to assess electricity users' contributions to grid peak loads: A case study. *Energy Oxford* 2024;288:129805. <http://dx.doi.org/10.1016/j.energy.2023.129805>.
- [26] de la Nieta AA, Ilieva I, Gibescu M, Bremdal B, Simonsen S, Gramme E. Optimal midterm peak shaving cost in an electricity management system using behind customers' smart meter configuration. *Appl Energy* 2021;283(December 2020):116282. <http://dx.doi.org/10.1016/j.apenergy.2020.116282>.
- [27] Hou Q, Yu Y, Du E, He H, Zhang N, Kang C, Liu G, Zhu H. Embedding scrapping criterion and degradation model in optimal operation of peak-shaving lithium-ion battery energy storage. *Appl Energy* 2020;278:115601.
- [28] Uddin M, Romlie MF, Abdullah MF, Tan CK, Shafiullah GM, Bakar AH. A novel peak shaving algorithm for islanded microgrid using battery energy storage system. *Energy* 2020;196:1–13. <http://dx.doi.org/10.1016/j.energy.2020.117084>.
- [29] Flygare C, Wallberg A, Hjalmarsson J, Fjellstedt C, Aalhuizen C, Castellucci V. The potential impact of a mobility house on a congested distribution grid – a case study in Uppsala, Sweden. In: *CIREC 2022*. 2022, p. 1079–83. <http://dx.doi.org/10.1049/icp.2022.0880>.
- [30] Kucevic D, Semmelmann L, Collath N, Jossen A, Hesse H. Peak shaving with battery energy storage systems in distribution grids: A novel approach to reduce local and global peak loads. *Electricity* 2021;2(4):573–89. <http://dx.doi.org/10.3390/electricity2040033>.
- [31] Castellucci V, Wallberg A, Flygare C. Potential of load shifting in a parking garage with electric vehicle chargers, local energy production and storage. *World Electr Veh J* 2022;13(9). <http://dx.doi.org/10.3390/wevj13090166>.
- [32] Wallberg A, Flygare C, Waters R, Castellucci V. Peak shaving for electric vehicle charging infrastructure—A case study in a parking garage in Uppsala, Sweden. *World Electr Veh J* 2022;13(8). <http://dx.doi.org/10.3390/wevj13080152>.